

Original Research

Chitosan-Based Conduits with Different Inner Diameters at both Ends Combined with Modified Formula Radix Hedysari Promote Nerve Transposition Repair

Fengshi Zhang^{1,2,3,†}, Qicheng Li^{1,2,3,†}, Bo Ma^{1,2,3}, Meng Zhang^{1,2,3}, Yuhui Kou^{1,2,3,*}¹Department of Orthopedics and Trauma, Peking University People's Hospital, 100044 Beijing, China²Key Laboratory of Trauma and Neural Regeneration, Peking University, 100044 Beijing, China³National Center for Trauma Medicine, 100044 Beijing, China*Correspondence: yuhui kou@bjmu.edu.cn (Yuhui Kou)

†These authors contributed equally.

Academic Editor: Jessica Amber Jennings

Submitted: 21 June 2023 Revised: 26 July 2023 Accepted: 8 August 2023 Published: 24 November 2023

Abstract

Background: Severe peripheral nerve injuries, such as deficits over long distances or proximal nerve trunk injuries, pose complex reconstruction challenges that often result in unfavorable outcomes. An innovative approach to repairing severe peripheral nerve damage involves using conduit suturing for nerve transposition repair. Cylindrical nerve guides are typically unsuitable for nerve transposition repair. Moreover, postsurgical adjuvant treatment is essential to promote the development of axonal lateral sprouts, proximal growth, and the restoration of neurostructure and function. The purpose of this research is to assess the impact of chitosan-based conduits with varying inner diameters on nerve transposition repair when combined with modified formula Radix Hedysari (MFRH). **Methods:** Using chitosan, we created conduits with varying inner diameters on both ends. These conduits were then utilized to repair the distal common peroneal and tibial nerves in SD rats using the proximal common peroneal nerve. Subsequently, MFRH was employed as a supplementary treatment. The assessment of the repair's effectiveness took place 16 weeks postsurgery, utilizing a range of techniques, including the neurological nerve function index, neuroelectrophysiological measurements, muscle wet weight, and examination of nerve and muscle histology. **Results:** The outcomes of our study showed that following 16 weeks of postoperative treatment, MFRH had a significant positive impact on the recovery of neuromotor and nerve conduction abilities. Moreover, there was a significant increase in the ratio of wet weight of muscles, cross-sectional area of muscle fibers, quantity and structure of regenerated myelinated nerve fibers, and the count of neurons. **Conclusions:** A combination of chitosan-based chitin conduits possessing different inner diameters and MFRH can considerably promote the regeneration and functional recovery of damaged nerves, which in turn enhances nerve transposition repair efficacy.

Keywords: peripheral nerve injury; nerve transposition; chitin; chitosan; peripheral nerve conduits

1. Introduction

Severe disability can result from damage to peripheral nerves [1,2]. Injuries to peripheral nerves can range in severity, with the destruction of nerves closer to the center and long-segment nerve deficits being particularly severe. For this level of nerve injury, recovery of nerve function is usually poor [3,4]. The long distance between the regenerated axons and the distal endorgans compromises the ability of motor neurons to regenerate axons into the distal stumps. As the nerves regenerate and grow further away, the muscles that correspond to them may slowly waste away, leading to the inability to receive the regenerating nerves. Despite the arrival of regenerated axons at the neuromuscular junction, their inability to reestablish function is attributed to the endorgans' incapacity to undergo reinnervation [5,6]. Therefore, optimal functional recovery requires nerve reinnervation within a shorter time after injury.

Peripheral nerve injury causes axons to sprout more lateral buds than themselves. The buds extend distally, pass

through the endoneural tube, and eventually grow into the target organ. The proximal fibers produce a significantly larger amount of lateral buds compared to both proximal fibers and distal endoneurial tubes, which is referred to as the nerve amplification effect [7,8]. This means that relatively thinner nerves can be used to repair relatively thicker damaged nerves and achieve a certain degree of functional recovery [9,10].

During nerve transposition repair, the challenge of suturing during surgery may become more difficult if there is a significant disparity in diameter between the proximal and distal nerves. To address this issue, the use of conduit suturing has emerged as a hopeful method for treating damage to peripheral nerves [11]. In the realm of neural tissue engineering, the creation of appropriate conduits for nerve restoration holds great significance. Numerous studies have been conducted on chitosan and chitin [12,13], which are among the various compounds utilized in the formulation of nerve conduits. Chitosan exhibits numerous outstanding



characteristics, including biocompatibility, biodegradability, antimicrobial attributes, and multifunctionality, which render it a highly promising substance within the realm of biomedicine. Its applications in drug delivery, wound healing, tissue engineering, and as a hemostatic agent give it significant advantages in medical therapy. In addition, chitosan is derived from chitin, which is readily available from crustacean waste, making it a cost-effective and renewable resource [14,15]. Most importantly, chitosan is an excellent material for preparing nerve conduits [16–18]. Several studies have indicated that chitosan and chitin could potentially engage with the microenvironment of nerve regeneration, leading to a decrease in neuroma incidence and enhancement of axon regeneration [19,20]. Our research group has recently used chitosan as the main component in manufacturing chitin conduits. These conduits demonstrate exceptional biocompatibility and mechanical properties. Instead of directly suturing the repaired nerve stumps, conduit suturing involves suturing them separately through the conduit in which they are sleeved [21]. Nevertheless, despite employing the technique of conduit suturing, a predicament persists where the outer diameter of the nerve fails to align with the inner diameter of the cylinder-shaped conduit. Using chitosan as a raw material, a conduit with different diameters at both ends was created for the treatment of tibial nerve injuries in rats. The conduit allowed successful tension-free suturing, nerve regeneration, and functional recovery through proximal transposition of the common peroneal nerve, leading to positive outcomes [22]. However, it remains uncertain whether the chitin conduit with varying diameters on each end, is appropriate for simultaneous repair of multiple distal nerves.

The process of nerve regeneration is complex and involves multiple mechanisms, cells, and factors [23]. Treating peripheral nerve injury with single-factor adjuvant therapy solely focuses on a single element of the intricate pathological mechanisms, which could potentially yield unsatisfactory results. Local treatments often fail to produce the good therapeutic effects due to the participation of the entire body in nerve regeneration [24]. Traditional Chinese medicines, known as multicomponent complexes, have the potential to create an optimal microenvironment for the regeneration of nerves through the stimulation of various biologically active substances [25]. The nerve amplification effect and regeneration were promoted by using Modified Formula Radix Hedysari (MFRH), a Traditional Chinese Medicine containing Radix Hedysari, *Epimedium*, and *Lumbricus*, for repairing tibial nerve injury in rats through proximal transposition of the common peroneal nerve, as demonstrated in our study [26]. Nonetheless, it remains uncertain whether MFRH can be employed for the simultaneous repair of multiple damaged nerves.

For this research, we initially employed chitosan to fabricate a conduit with varying inner diameters on both ends. Subsequently, we investigated the impact of employ-

ing this conduit and MFRH therapy in the simultaneous restoration of numerous distal nerves for nerve recovery. Various methods were used to evaluate the success of the repair, including the neurological nerve function index, neuroelectrophysiological measurements, muscle wet weight, and examination of nerve and muscle histology.

2. Materials and Methods

2.1 Statement on Ethical Principles

The animal protocols and treatment followed the Guidelines for Ethical Review of Experimental Animals for Animal Welfare, as outlined by the Ethics Committee and Experimental Animal Center of Peking University People's Hospital in Beijing, China. The study obtained an approved permit, with permit number 2022PHE050. Animal surgeries and care adhered to the standards of the National Institutes of Health Guide for the Care and Use of Laboratory Animals (NIH Publication No. 85-23, revised 1985). Information about the animals was displayed in accordance with the ARRIVE 2.0 guidelines.

2.2 Preparation of Chitin Conduits with Varying Inner Diameters on Each End

The manufacturing mold used for the conduit is made entirely of stainless steel. The mold consists of two cylindrical guiding rods with varying diameters that are connected by a conical piece. The thinner guiding rod has a diameter of 0.8 mm, while the thicker guiding rod measures 1.8 mm in diameter. The conical piece's diameters on both ends match the diameter of the guiding rods on both sides. The guiding rod diameter is crucial in shaping the conduit, as it determines the final output size and shape.

The chitin conduits were constructed using previously described methods [27]. To prepare a 4% (w/v) chitosan solution, chitosan (Beijing Chemical Factory, Beijing, China) with a deacetylation level exceeding 70% and a molecular weight ranging from $15\text{--}50 \times 10^4$ Da was dissolved in an aqueous solution of 2% acetic acid (Beijing Chemical Factory, Beijing, China). The bubbles in the solution were removed using a vacuum pump. The particular mold was gradually submerged in a solution of chitosan, ensuring that the mold's surface was uniformly coated with the chitosan solution. Subsequently, it was immersed in an aqueous solution of NaOH (Beijing Chemical Factory, Beijing, China) to solidify the chitosan solution on the mold's surface. The remaining NaOH was rinsed off with purified water, followed by the use of acetone to remove moisture from the chitosan. Afterwards, chitosan underwent acetylation using acetic anhydride (Beijing Chemical Factory, Beijing, China) to create chitin conduits that possessed varying inner diameters on both extremities. Afterwards, the conduits were delicately removed from the mold and placed in a solution containing 75% ethanol (Beijing Chemical Factory, Beijing, China) for future utilization (Fig. 1).

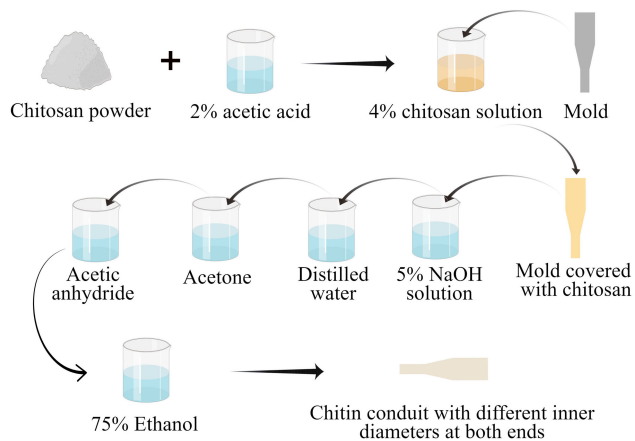


Fig. 1. The process of preparing chitin conduits with varying inner diameters on both ends.

2.3 Drug Preparation

MFRH was prepared using previously described methods [26]. Gansu Province, China, was the place of origin for *Radix Hedysari* and *Epimedium*, whereas Guangdong Province, China, was the place of origin for *Lumbricus*. All of them were purchased in Beijing, China. First, *Radix Hedysari*, *Epimedium*, and *Lumbricus* were boiled with distilled water for 2 hours and then for 1 hour. After that, the combined liquid was condensed to a concentration of 1 g/mL (equal to the weight of the dried plant material) and stored at 4 °C until needed. Saline was used to dissolve mecobalamin (Aladdin, Shanghai, China).

2.4 Experimental Animal Preparation

We bought 36 female specific-pathogen-free Sprague-Dawley rats from Beijing Vital River Laboratory Animal Technology Co., Ltd., China (license No. SCXK (Jing) 2021-0006). The rats, which were six weeks in age and had a weight ranging from 200 to 220 g, were kept at the Experimental Animal Center located in Peking University People's Hospital. The rats were housed in a controlled environment maintained at a temperature of 24 °C, with a relative humidity ranging from 50% to 55% and a light/dark cycle of 12 hours each. The rats were given unrestricted access to regular pellet food and fresh water. The rats were divided into four groups ($n = 9$ per group) in a random manner. These groups included the sham group, the negative control group, the MFRH group and the positive control group. In the negative control group, MFRH group and positive control group, the distal common peroneal and tibial nerves were repaired using the common proximal peroneal nerve. In the sham group and negative control group, rats received oral administration of a sterile saline solution after surgery. In the MFRH group, rats received oral administration of MFRH after surgery. In the positive control group, rats received oral administration of mecobalamin after surgery. Following the administration of 2.5%

isoflurane (RWD, Shenzhen, China) using an animal anesthesia machine (RWD, Shenzhen, China), the right sciatic nerve of each rat was revealed by removing the hair on the lower right limb. After the surgery, the rats were administered pain-preventing jelly (NEWLOONG LIFE SCITECH, Shanghai, China). Daily, the animals were closely monitored, and if any indications of self-harm were identified, a solution of picric acid (MilliporeSigma, Burlington, MA, USA) was administered to prevent deterioration. All measures were taken to reduce animal suffering, and the study followed ethical protocols.

2.5 Nerve Injury and Repair Model

To reveal the sciatic nerve and its two main divisions (namely, the common peroneal nerve and the tibial nerve), surgical operations were carried out on the right sciatic nerves. Standard microsurgical techniques were employed under aseptic conditions, utilizing a surgical microscope for all surgical procedures. To reduce tension on the repair site, a technique called the dorsal gluteal-splitting approach was employed, which involved gentle dissection of the nerve branches.

Transection of the common peroneal nerve and tibial nerve occurred at a distance of five millimeters from the bifurcation in the saline, MFRH, and mecobalamin groups. The tibial nerve's proximal stump was surgically treated using 10-0 nylon sutures (Lingqiao, Ningbo, China), and then it was connected to a nearby muscle. The repair involved the proximal end of the common peroneal nerve, as well as the distal ends of both the common peroneal nerve and the tibial nerve. Approximately 2 mm into the thinner end of the conduit, the proximal stump of the common peroneal nerve was inserted. Approximately 2 mm deep, the thicker end of the conduit received the distal stumps of both the common peroneal nerve and the tibial nerve. A 2-mm space was maintained between the proximal stump and the distal stumps, and the stumps were secured to the conduit using a 10-0 nylon suture. In the end, the surgical area was closed using 4-0 nylon sutures (Lingqiao, Ningbo, China) in layers (Fig. 2).

In the sham group, we revealed the sciatic nerve and its branches without inducing any harm to the nerve fibers. Afterward, the surgical area was carefully stitched using 4-0 nylon in multiple layers.

2.6 Drug Treatment

After the surgical operation, every rat in the sham and saline groups was given 2 mL of sterile saline solution via oral gavage every day, beginning from the day following the surgery. In the meantime, every rat in the MFRH group received a daily dosage of 2 mL of MFRH (1 g/mL). Every rat in the mecobalamin group received a dosage of 2 mL of liquid mecobalamin (100 µg/kg). Oral gavage lasted for a period of 16 weeks.

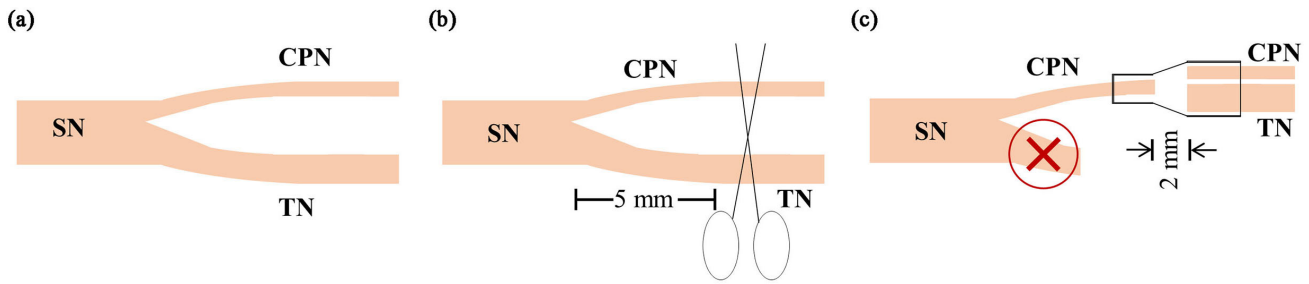


Fig. 2. Schematic diagram of surgical procedures. (a) The sciatic nerve and its two primary divisions are known as the common peroneal nerve and the tibial nerve. (b) The tibial nerve and the common peroneal nerve were cut 5 mm away from the point where they split into two branches. (c) The nearby end of the common peroneal nerve was utilized for the restoration of the distal end of both the common peroneal nerve and the tibial nerve. CPN refers to the common peroneal nerve, SN stands for the sciatic nerve, and TN represents the tibial nerve.

2.7 General and Local Conditions of Rats after Operation

Following the surgery, the rats were provided with regular nourishment, and their daily progress was meticulously documented, encompassing their food intake, physical movement, recovery of the surgical incision, and mobility of the operated limb. After a period of sixteen weeks following the surgical procedure, the common peroneal nerve and tibial nerve that had been repaired were uncovered, allowing for examination of the nerve's structure and the presence of any adhesions in the surrounding tissue.

2.8 Neurological Function Index

The Rat and Mouse Gait Analysis Processing System v1.09 (Zhongshi Dichuang Technology, Beijing, China) was utilized to assess the restoration of motor function at the 16-week postoperative period. Each rat was strolled along a sealed passageway made up of a transparent floor and walls made of dark synthetic material. The sciatic functional index (SFI) was computed using the formula we supplied [28].

$$SFI = \frac{109.5(ETS - NTS)}{NTS} - \frac{38.3(EPL - NPL)}{NPL} + \frac{13.3(EITS - NITS)}{NITS} - 8.8$$

ETS represents the distance between the first and fifth toes of the right hind limb, while NTS represents the same distance for the left hind limb. EPL measures the distance from the heel to the top of the third toe of the right hind limb, and NPL measures the distance from the heel to the top of the third toe of the left hind limb. Additionally, EITS represents the distance between the second and fourth toes of the right hind limb, and NITS represents the same distance for the left hind limb.

2.9 Nerve Electrophysiological Detection

After 16 weeks of surgery, a MedlecSynergy electrophysiological device (04oc003, Oxford Instrument Inc., Abingdon, UK) was used to assess the recovery of regenerated nerve conduction on the right side in every rat. Under 2.5% isoflurane anesthesia (RWD, Shenzhen, China), the tibial nerve on the right side and the gastrocnemius muscle were carefully exposed. Stimulation occurred at the proximal and distal terminals of the tibial nerve, while recording took place at the center of the gastrocnemius muscle. Recordings were made of the magnitude and delay of the compound muscle action potential (CMAP), followed by the calculation of nerve conduction velocity using the subsequent procedure. The conduction velocity of the tibial nerve was determined by calculating the ratio of the length of the nerve trunk (dl) to the difference in action potential latency (dt) between proximal and distal tibial nerve stimulation.

2.10 Immunofluorescence Staining of Regenerated Nerve Fibers

At 16 weeks postoperatively, the distal tibial nerve was obtained after euthanizing the rats using carbon dioxide. The nerve was treated with 4% paraformaldehyde (Solarbio, Beijing, China) for 24 hours and subsequently sectioned into transverse slices measuring 12 μ m in thickness utilizing a frozen slicer. Immunofluorescence staining was performed according to a well-established protocol [29]. The NF200 primary antibody (1:400, MilliporeSigma, Burlington, MA, USA) was used to monitor the regeneration of axons, while the S100 primary antibody (1:400, MilliporeSigma, Burlington, MA, USA) was used to identify Schwann cells. In short, sections of nerve tissue were treated with primary antibodies that targeted NF200 and S100 overnight at 4 $^{\circ}$ C. Subsequently, they were washed with phosphate buffered saline (PBS). Afterwards, a secondary antibody labeled with Alexa488 (1:500, Abcam, Cambridge, UK) and a secondary antibody labeled with Alexa594 (1:500, Abcam, Cambridge, UK) were

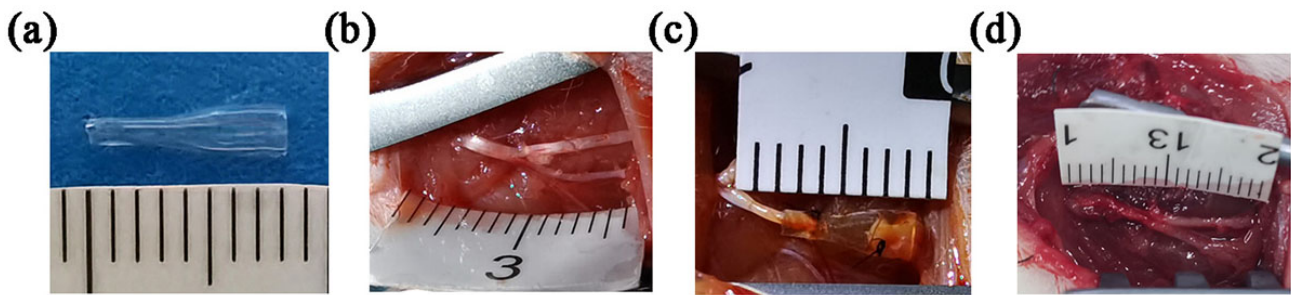


Fig. 3. Chitin conduit and nerve transposition repair. (a) Gross view of the chitin conduit displaying varying inner diameters on both ends. (b) The prototype of the sciatic nerve and its branches. (c) Representative image of nerve transposition repair. (d) Representative photograph of the repaired nerve at 16 weeks postoperatively.

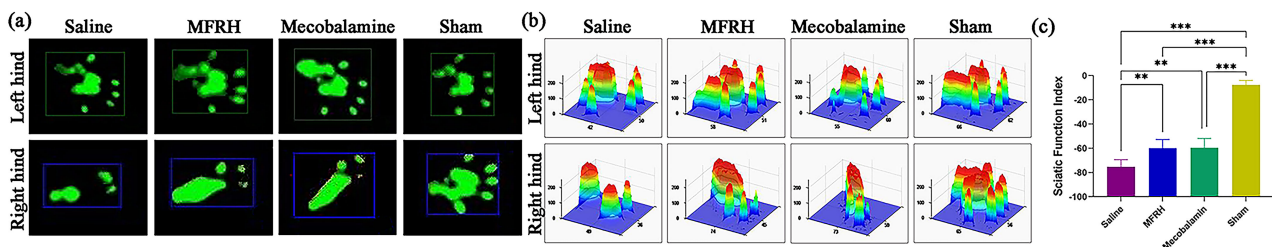


Fig. 4. Motor function assessment at 16 weeks after operation. (a) Representative footprints. (b) Representative three-dimensional stress diagrams. (c) The sciatic functional index (SFI) in each group. Data are presented as the mean \pm standard deviation (SD). ** $p < 0.01$; *** $p < 0.001$.

added and incubated at room temperature for 1 hour. DAPI was used to stain the nucleus for a duration of 5 minutes. The sections were observed by 3D Fluorescence Imaging System (HOOKE INSTRUMENTS, Changchun, China).

2.11 Evaluation of the Morphological Characteristics of Regenerated Nerve Fibers

At 16 weeks postoperatively, the distal tibial nerve was obtained after euthanizing the rats using carbon dioxide. An established protocol was used to perform morphological assessment of regenerated nerve fibers [29]. The nerve tissue was treated with 2.5% glutaraldehyde for a duration of 24 hours and then subjected to staining using 1% osmic acid (Electron Microscopy Sciences, Hatfield, PA, USA). To prepare the sample, a gradient concentration of acetone was utilized for dehydration. Afterwards, the specimens were immersed in epoxy resin and then cut into semithin slices measuring 700 nm in thickness, and ultrathin slices measuring 70 nm in thickness. The semithin sections were stained using a 1% solution of toluidine blue (Solarbio, Beijing, China) and examined with an optical microscope (Olympus Corporation, Tokyo, Japan), to compute the nerve fiber density. The ultrathin slices were treated with uranyl acetate and lead citrate (Electron Microscopy Sciences, Hatfield, PA, USA) and examined under a transmission electron microscope (Olympus Corporation, Tokyo, Japan). ImageJ software (version 1.8.0, LOCI, University of Wisconsin, Madison, WI, USA) was

utilized to measure the diameters of the axons and nerve fibers. Myelin thickness was calculated with the formula (fiber diameter - axon diameter) divided by 2.

2.12 Target Muscle Recovery

At 16 weeks following the surgical procedure, the gastrocnemius muscles were gathered from both sides, and their weights were measured. The wet weight ratio of the gastrocnemius muscles was calculated by dividing the wet weight of the muscle on the right side by the wet weight of the muscle on the left side. Next, the muscles on the right side were immobilized in 4% paraformaldehyde at 4 °C for the entire night. Afterward, they were encased in paraffin and sliced into 6- μ m-thick sections. Afterwards, Masson's trichrome stain was applied to the sections, and random images of the muscle cross-section were taken from five fields in each image. ImageJ software was used to measure the cross-sectional area of the muscle fibers in these images. Afterwards, the wet weight proportion and average cross-sectional area of the gastrocnemius muscle fibers on the right side were computed and compared across the four groups.

2.13 Fluor-Gold (FG) Retrograde Tracing

After a period of sixteen weeks following the surgical procedure, the nerves of the rats were revealed through the initial cut while being administered 2.5% isoflurane anesthesia. The proximal end of the common peroneal nerve

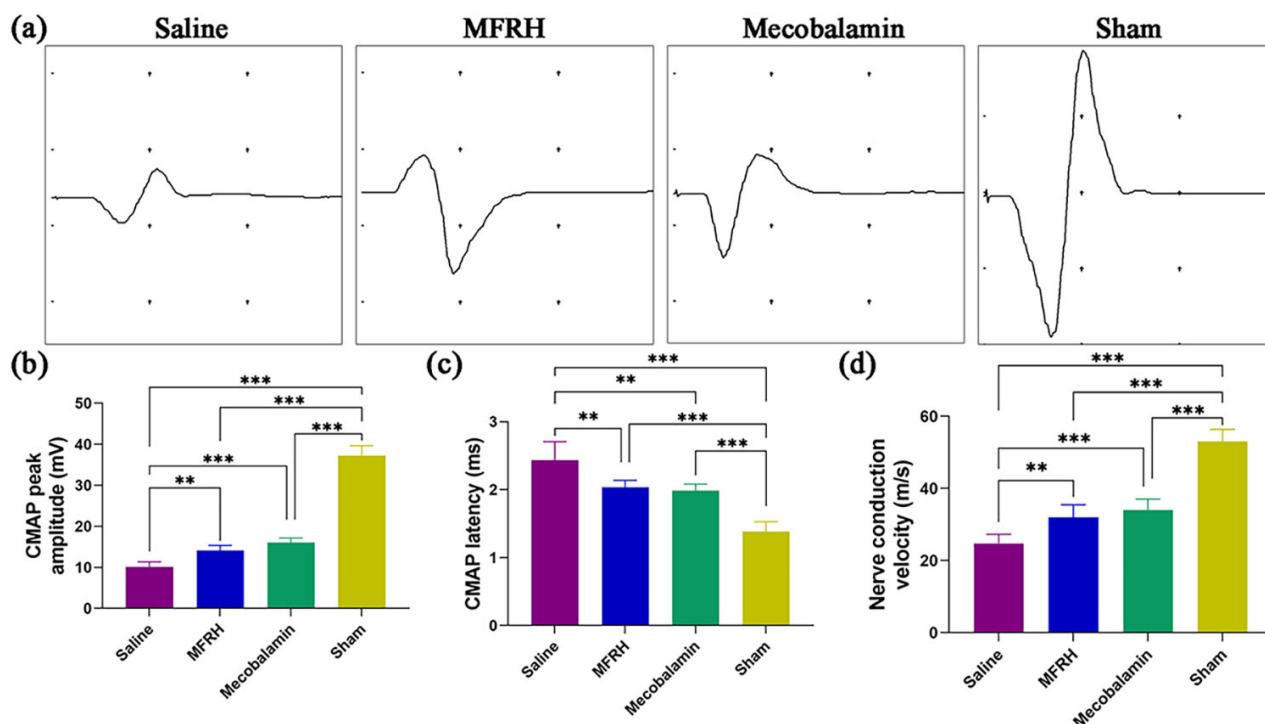


Fig. 5. Nerve electrophysiological evaluation 16 weeks after the operation. (a) Representative compound muscle action potential (CMAP) waveform. (b) Statistical examination of peak amplitudes in CMAP. (c) Statistical analysis of the latency of CMAP. (d) Statistical examination of the velocity of nerve conduction. Data are presented as the mean \pm SD. ** $p < 0.01$; *** $p < 0.001$. The data are displayed as the average plus standard deviation. p value less than 0.01; p value less than 0.001.

was injected with a 4% FG (Fluorochrome, Denver, CO, USA) solution, after which the incision was sutured. Following a week, the rats were immobilized using a solution of 0.9% NaCl and 4% paraformaldehyde by means of transcardiac perfusion while being anesthetized. After that, the spinal cord from L4–L6 and the dorsal root ganglia (DRG) were extracted and then treated with a 4% paraformaldehyde solution at a temperature of 4 °C for 12 hours. Following this, they were dehydrated using sucrose solutions with varying concentrations (starting from 10% and gradually increasing to 20% and then to 30%). Then, the specimens were sequentially sectioned following embedding in optimum cutting temperature (OCT) compound (Sakura, Torrance, CA, USA). The spinal cord samples were cut into sections that were 25- μ m-thick, while the DRG samples were cut into sections that were 20- μ m-thick. To quantify the number of anterior horn motor neurons in the spinal cord and DRG sensory neurons after regeneration in response to each treatment, the sections were examined using the 3D Fluorescence Imaging System (HOOKE INSTRUMENTS, Changchun, China).

2.14 Statistical Analysis

Both image analysis and behavior assessments in the study were conducted using a blinded method. The mean and standard deviation (SD) were used to present the results. SPSS 22 (IBM Corp., Armonk, NY, USA) was uti-

lized for the statistical analysis. Multiple groups were compared using one-way analysis of variance (ANOVA). If there was a notable distinction between groups, the Tukey post hoc test was utilized to conduct pairwise comparisons. A p value of less than 0.05 was chosen as the level of significance.

3. Results

3.1 General Observation

As depicted in Fig. 3a, the conduit is transparent. The two ends of the conduit have different inner diameters. The thinner end has an inner diameter of 0.8 mm, while the thicker end has an inner diameter of 1.8 mm. A conical structure connects the narrower and wider ends. The prototype of the sciatic nerve and its branches is depicted in Fig. 3b. As depicted in Fig. 3c, the diameter of the nerves matches the inner diameter of the conduit. As depicted in Fig. 3d, at the 16-week mark following the surgery, the conduit underwent partial absorption, with no apparent signs of inflammation or neuroma detected at the nerve suture location.

3.2 Neurological Function Index

At 16 weeks postsurgery, a functional index analysis was conducted on each group to evaluate the recovery of motor function. The results are depicted in Fig. 4. Specif-

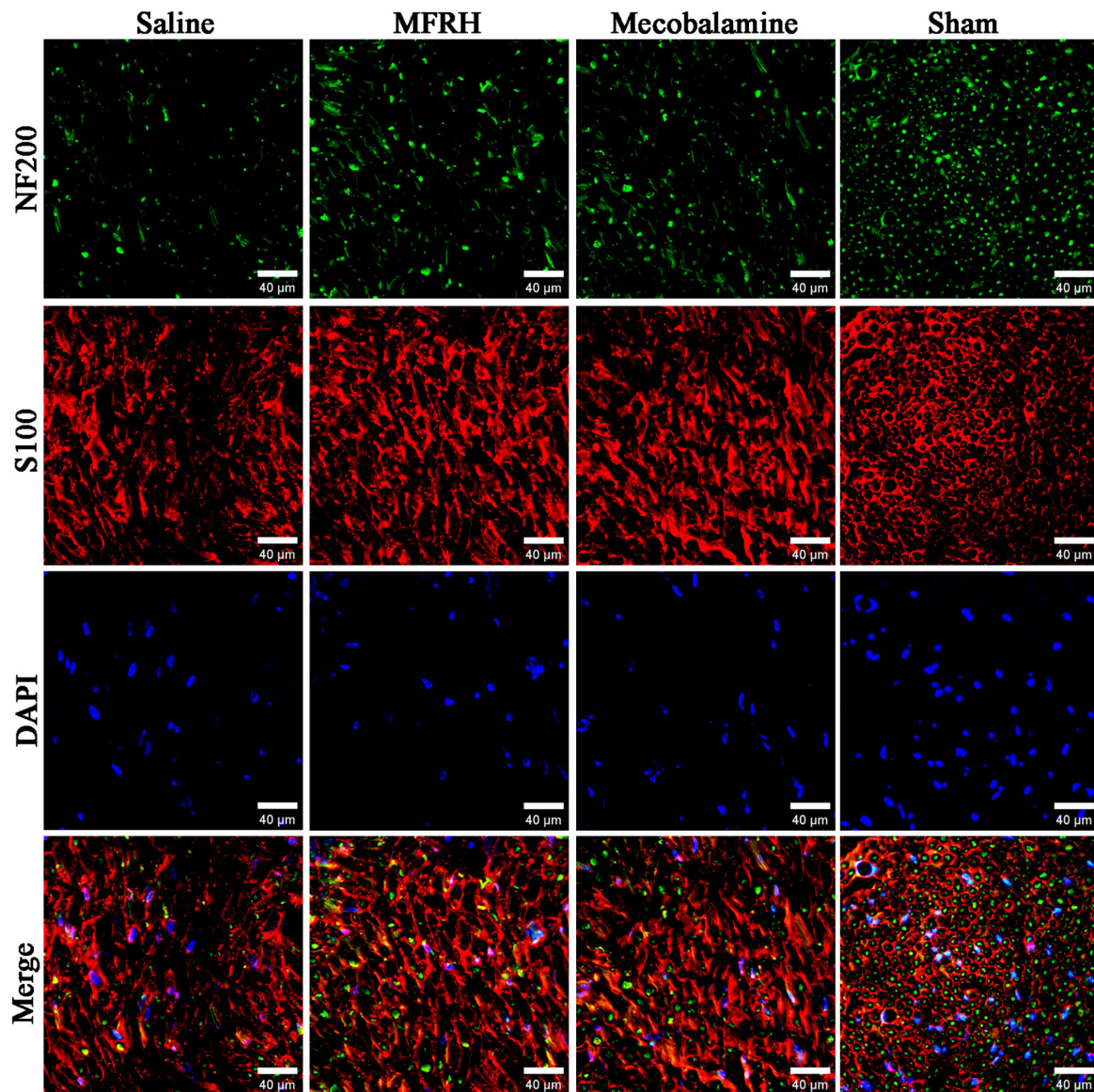


Fig. 6. Illustrative pictures showing the immunofluorescence staining of newly formed nerve tissue. The presence of nuclei is revealed by blue fluorescence, Schwann cells are represented by red fluorescence, and regenerating axons are indicated by green fluorescence. Scale bar = 40 µm.

ically, Fig. 4a displays the typical footprints, and Fig. 4b displays the three-dimensional stress diagrams. The SFI of each group is displayed in Fig. 4c. Both the SFI of the MFRH group and the mecobalamin group were significantly higher than that of the saline group ($p < 0.01$) but significantly lower than that of the sham group ($p < 0.001$). However, there was no significant difference observed between the MFRH group and the mecobalamin group.

3.3 Electrophysiological Detection of Nerves

At the 16th week after surgery, rats from each group underwent electrophysiological tests to ascertain nerve conduction recovery, as revealed in Fig. 5. The amplitude of CMAP is positively associated with the quantity of innervated muscle fibers, while the latency of CMAP is inversely

correlated with the thickness of the myelin sheath surrounding the nerve fibers. Fig. 5a demonstrates typical CMAP waveforms for each rat group. In Fig. 5b, in comparison to the sham group, both the MFRH and mecobalamin groups exhibited significantly reduced CMAP peak amplitudes ($p < 0.001$), yet they displayed significantly elevated CMAP peak amplitudes when compared to the saline group ($p < 0.01$). Furthermore, there was no notable distinction observed between the MFRH and mecobalamin cohorts. In addition, the MFRH and mecobalamin groups exhibited a significantly higher CMAP latency than the sham group ($p < 0.001$) but a significantly lower CMAP latency than the saline group ($p < 0.01$), as depicted in Fig. 5c. Furthermore, there was no notable distinction observed between the MFRH and mecobalamin groups. Fig. 5d indicated a

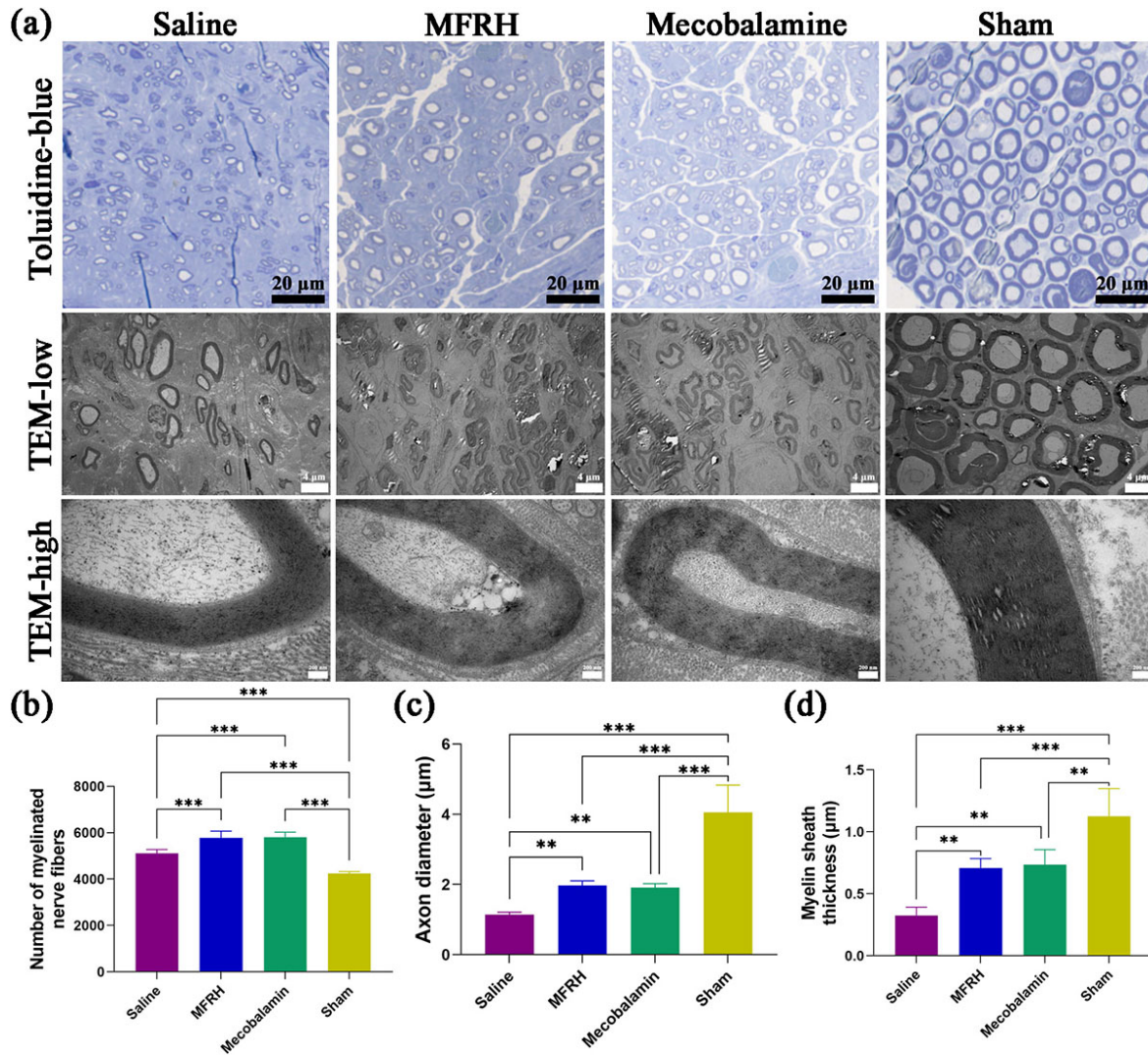


Fig. 7. Evaluation of the regenerated nerve fibers through histological analysis 16 weeks postsurgery. (a) Representative images of toluidine blue staining and transmission electron microscopy are shown. (b) Statistical examination of the quantity of regenerated axons for each group. (c) Statistical examination of the diameter of axons in the regenerated nerve. (d) Statistical analysis on the thickness of the myelin sheath in the regenerated nerves within each group. Data are displayed as the mean \pm SD. ** $p < 0.01$; *** $p < 0.001$.

significant decrease in nerve conduction velocity in both the MFRH and mecobalamin groups compared to the sham group ($p < 0.001$), but the reduction was even more pronounced in the saline group ($p < 0.01$). The MFRH and mecobalamin groups did not show any notable distinction.

3.4 Immunofluorescence Staining of Regenerated Nerve Tissue

Immunofluorescence staining was conducted on the cross-sections of the regenerated nerves of rats in all groups at the 16th week following the nerve surgery, and the findings are illustrated in Fig. 6. The presence of nuclei is revealed by blue fluorescence, Schwann cells are represented by red fluorescence, and regenerating axons are indicated by green fluorescence. The findings indicated that both the MFRH group and the mecobalamin group exhibited higher axonal regeneration than the saline group.

3.5 Evaluation of the Morphological Characteristics of Regenerated Nerve Fibers

Fig. 7 displays the findings from toluidine blue staining and electron microscopy analysis of the cross section of the regenerated nerve. Fig. 7a shows representative images of staining with toluidine blue and transmission electron microscopy. The uniformity of regenerated myelinated nerve fibers in the saline, MFRH, and mecobalamin groups was lower than that in the sham group. According to the findings, the MFRH and mecobalamin groups exhibited a notably greater quantity of myelinated nerve fibers than the saline and sham groups ($p < 0.001$). Additionally, the saline group had a significantly higher tally than the sham group ($p < 0.001$) (Fig. 7b). Fig. 7c demonstrates the diameter of the regenerated nerves' axon. The axon diameter of both the MFRH and mecobalamin groups was significantly

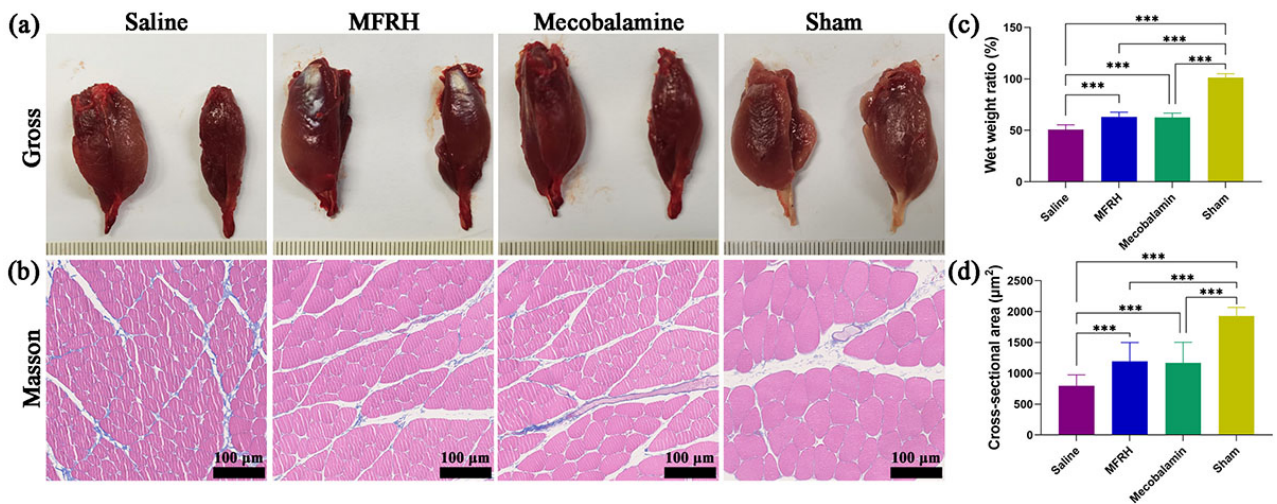


Fig. 8. Evaluation of the gastrocnemius muscle through histological analysis 16 weeks postsurgery. (a) Illustrative pictures showcasing the unaffected (on the left) and damaged (on the right) gastrocnemius muscles. (b) Representative pictures displaying Masson staining of the right gastrocnemius muscle in every group. (c) Analyzing the statistical ratio of wet weight in every group. (d) The groups were analyzed statistically to determine the average cross-sectional area of muscle fibers in terms of cross-sectional area. The data are displayed as the mean \pm SD. *** $p < 0.001$.

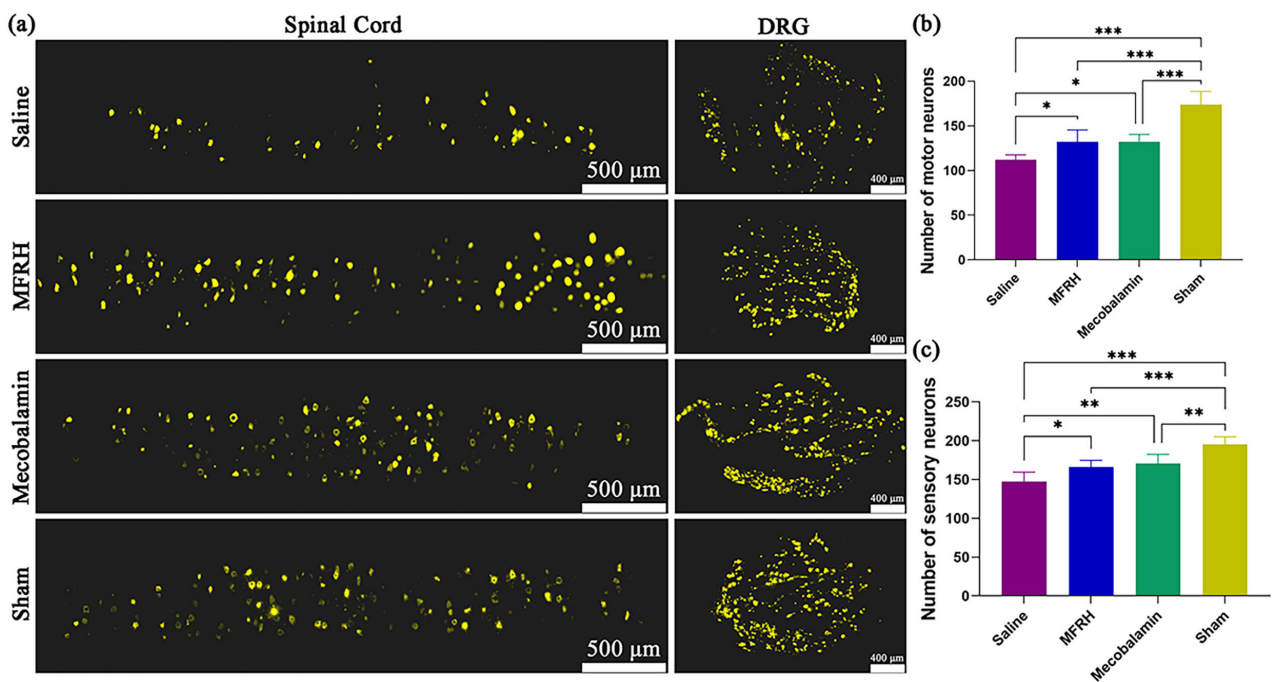


Fig. 9. FG retrograde tracing of neurons at 16 weeks after operation. (a) Representative pictures of neurons labeled with FG in every group. (b) Statistical analysis was conducted on the quantity of motor neurons labeled with FG in every group. (c) Statistical analysis of the quantity of sensory neurons labeled with FG in every group. The data are displayed as the mean \pm SD. * $p < 0.05$; ** $p < 0.01$; *** $p < 0.001$.

higher than that of the saline group ($p < 0.01$) but significantly lower than that of the sham group ($p < 0.001$). There was no significant difference observed between the MFRH group and the mecobalamin group. The myelin sheath thickness of the regenerated nerves in each group was displayed by Fig. 7d. There was no notable distinction be-

tween the MFRH group and the mecobalamin group; however, both groups exhibited a considerably greater thickness than the saline group ($p < 0.01$). Additionally, both groups demonstrated a significantly lower thickness than the sham group ($p < 0.01$).

3.6 Gastrocnemius Muscle Recovery

At 16 weeks following the surgical procedure, both gastrocnemius muscles were obtained from rats, weighed, photographed, and subjected to Masson staining specifically on the right side. The obtained results from the procedure are illustrated in Fig. 8. Fig. 8a shows illustrative pictures of the gastrocnemius muscles on both the left and right sides for every group, whereas Fig. 8b shows the staining results of the right gastrocnemius muscle for each group. The findings indicated that the wet weight ratio of the gastrocnemius muscles on the right and left sides was notably reduced in both the MFRH and mecobalamin groups in comparison to the sham group ($p < 0.001$). Nevertheless, they exhibited a greater value compared to the saline group ($p < 0.001$). The MFRH group and the mecobalamin group showed no notable distinction (Fig. 8c). Moreover, as exhibited in Fig. 8d, in the MFRH group and the mecobalamin group, the average cross-sectional area of muscle fibers was significantly smaller than that in the sham group ($p < 0.001$) but notably larger than that in the saline group ($p < 0.001$).

3.7 FG Retrograde Tracing

As depicted in Fig. 9, after a period of 16 weeks following the operation, the FG retrograde tracing technique was utilized to assess the quantity of motor neurons in the front horn of the spinal cord and sensory neurons in the DRG of every group. The analysis of the results was conducted to assess the level of nerve regeneration in every group. As depicted in Fig. 9a, in each group, motor neurons and sensory neurons labeled with FG were observed. The quantity of motor neurons labeled with FG in the MFRH and mecobalamin groups exhibited a significant increase compared to the saline group ($p < 0.05$), yet it was notably lower than the motor neurons in the sham group ($p < 0.001$). No notable distinction was observed between the MFRH and mecobalamin groups (Fig. 9b). The quantity of sensory neurons labeled with FG in the MFRH and mecobalamin groups exhibited a significant increase compared to that in the saline group ($p < 0.05$), yet it was notably lower than that in the sham group ($p < 0.01$). Nevertheless, there was no notable distinction observed between the MFRH and mecobalamin cohorts (Fig. 9c).

4. Discussion

Different degrees of severity exist in peripheral nerve injuries, with long-distance nerve deficits and proximal nerve trunk injuries being especially severe [30,31]. The limited improvement in nerve function is a result of the challenge in regenerating axons to extend to the distant stump and the deterioration of the target organ during this process [32,33]. Hence, to enhance the effect of nerve restoration, it is crucial to promptly re-establish innervation in the target organs.

An amplification effect during the process of nerve regeneration has been recorded in previous research [7,21].

During the initial phases of nerve recovery after being injured, a nerve fiber develops numerous side branches and stretches toward the distal endoneural tubes [34,35]. When there are more distal endoneural tubes than proximal nerve axons, there is sufficient room for regenerated axons to develop [36,37]. The amplification phenomenon could potentially be utilized as an innovative approach in the treatment of severe peripheral nerve damage. This involves the utilization of smaller nerves to repair thicker damaged nerves or the use of a single nerve to repair multiple nerve injuries at the same time. Nerve transposition repair involves the donor nerve sending additional sprouts to the distal stump. This helps to re-establish innervation to the target organ as early as possible, and promotes effective rehabilitation of neural structure and function [38,39]. This study utilized the common peroneal nerve to simultaneously repair the distal common peroneal nerve and tibial nerve. The nerve regeneration amplification effect was confirmed by the findings.

Over the past few years, researcher have developed several different methods to fix brachial plexus injuries, including the utilization of cervical spinal nerve 7 on the same/opposite side, the accessory nerve, and the phrenic nerve [4]. Additionally, they have repaired median nerve injury by using the musculocutaneous nerve [11] and fixed ulnar nerve injury by using the Pronator quadratus muscle branch [40]. The success of nerve transposition repair greatly depends on the skillful suturing of the nerve. Unlike the common suturing method used to treat nerve injuries, the diameters of the proximal and distal nerves are often not consistent in nerve transposition repair [41]. In this case, the epineurial suture may cause localized hypertension at the site of the suture. After repair, the suturing location might give rise to neuromas, leading to the occurrence of nerve pain [42]. Excessive local tension can hinder the proper growth of proximal nerves toward distal nerves, ultimately impacting nerve regeneration following transposed repair [43]. This study resolved the issue by utilizing the conduit suturing technique. By suturing the nerves at both ends with minimal tension, the occurrence of local neuromas and secondary neuralgia can be significantly reduced. Furthermore, the technique maintains the spaces between nerve stumps, and research has indicated that the regrowth of axons is associated with the distance separating the nerve stumps [29,44]. According to our previous findings, the optimal gap for nerve regeneration in rats is 1–2 mm [8,45]. The study found that there was a 2 mm gap, which had no impact on either the process or precision of nerve regeneration.

When utilizing conduits that have identical inner diameters on both ends to repair large nerves with small nerves or to repair multiple nerves with a single nerve, the following issues may arise. If the inner diameter of the conduit fits the proximal donor nerve, compression may occur on the distal recipient nerve. Conversely, if the inner di-

iameter of the conduit matches the distal recipient nerve, there may be an excessive gap between the inner wall of the conduit and the proximal donor nerve, leading to potential escape of more regenerated nerve fibers and an increased likelihood of neuroma formation. Hence, this investigation effectively addressed this issue by employing conduits with varying inner diameters on both ends. The thinner end of the conduit has an inner diameter of 0.8 mm, which fits the diameter of the proximal common peroneal nerve. The thicker end has an inner diameter of 1.8 mm, which matches the combined diameters of the distal common peroneal nerve and the tibial nerve. The conduit's inner diameter is slightly larger than the nerve's diameter, with a range of 0.1 to 0.2 mm, due to three primary factors. First, inserting the nerve into the conduit and performing a suture without tension is a simple task. Secondly, when the nerve is injured, there will be tissue swelling, which leads to an increase in the nerve's diameter. This allows for a perfect fit with the conduit's diameter, preventing obstruction of blood supply due to compression of the nerve tissue. Additionally, by populating the conduit with nerves, the leakage of regenerated nerve fibers will be reduced, effectively preventing the development of neuromas.

Chitosan served as the primary component for fabricating nerve conduits in this investigation. Currently, various biomaterials are used to prepare nerve conduits, and chitosan has received much attention from researchers. Chitosan exhibits numerous advantageous characteristics, such as biocompatibility, biodegradability, antimicrobial attributes, and multifunctionality, which render it a highly promising substance in the domain of biomedicine [15]. According to previous research, chitosan-based nerve conduits have been found to be advantageous in the restoration of peripheral nerves [13]. Successful repair is achieved by facilitating the smooth passage of regenerated nerve fibers across the gap toward the distal nerve, through the utilization of this conduit during peripheral nerve injury repair. The initial step of this research involved dissolving chitosan in acetic acid solution to create a chitosan solution. Next, the solution is uniformly applied to the surface of the personalized mold. Under the action of sodium hydroxide, the chitosan solution solidifies and forms a conduit. Subsequently, with the influence of acetic anhydride, the chitosan underwent acetylation, resulting in decreased hardness and enhanced elasticity, ultimately leading to the formation of the chitin conduit. This method is not only easy to operate but can also customize conduits of different specifications according to different conditions of nerve injury.

Although the utilization of conduits with different sizes at both ends for nerve transposition repair offers numerous advantages, it solely tackles the problem of surgical suturing, indicating the need for additional enhancements in the effectiveness of the repair process. Previous studies have suggested that the regeneration of injured nerves involves various mechanisms, cells, and factors. After sur-

gical suturing, certain additional treatments may induce the development of proximal axonal branches, promote the amplification effect, and ultimately facilitate the restoration distant nerves [46–48]. Repair of damaged nerves is an intricate procedure involving multiple mechanisms. Treating only one aspect is limiting and may not target the numerous pathologic mechanisms associated with peripheral nerve injury [49,50]. Several research studies have suggested that traditional Chinese medicine has the ability to create a conducive environment for nerve regeneration by activating different bioactive elements that are essential for the process of nerve regeneration [51,52]. In our earlier study, MFRH enhanced the amplification effect of the common peroneal nerve to repair the tibial nerve, and promote nerve repair [26]. Consequently, we selected MFRH as an auxiliary treatment approach to simultaneously fix several nerves with a single nerve in this study. Mecobalamin, a naturally occurring coenzyme B12, is commonly prescribed in clinical practice to treat peripheral neuropathy [53]. It has the ability to enhance axon transport function and promote axon regeneration. For this research, we utilized mecobalamin treatment as the positive control group, whereas saline treatment was used as the negative control group. The results showed that 16 weeks after surgery, MFRH significantly improved the recovery of neuromotor function and neurological conduction function. Moreover, there was a significant increase in the ratio of wet weight of muscles, cross-sectional area of muscle fibers, quantity and structure of regenerated myelinated nerve fibers, and the count of neurons. The study findings validated that MFRH plays a significant role in enhancing the amplification effect of peripheral nerves, facilitating the simultaneous repair of multiple nerves by a single nerve. It is important to mention that, in the nerve transposition repair, the target organ corresponding to the injured nerve needs to receive a new central innervation. While the regenerated nerve fibers can reach target organ for reinnervation, achieving true nerve repair necessitates remodeling of nerve functionality. This process is time-consuming and crucial in clinical nerve transposition repair [54–56]. Taking this into account, we decided to assess the rats 16 weeks after the operation.

The combination of Radix Hedysari, *Epimedium*, and *Lumbricus* in MFRH can potentially achieve treatment goals by utilizing various mechanisms. MFRH primarily consists of Radix Hedysari. For many years, Radix Hedysari has been known as a medicinal plant that exhibits a diverse array of biological and pharmacological effects. Polysaccharides, flavonoids, phenylpropanoids, and trace elements are some of the chemical constituents that have been isolated and identified from Radix Hedysari by researchers. One of the main components of Radix Hedysari is Hedysarum polysaccharides (HPS), which possess diverse biological functions, such as antioxidation, immune modulation, and regulation of intestinal flora, and is extensively employed in the treatment of numerous diseases [57–

63]. More importantly, HPS can relieve oxidative stress, has anti-apoptotic neuroprotective effects, and can be used to prevent or treat neurodegenerative diseases [64]. Our previous research revealed that, treating sciatic nerve crush injury in rats utilizing HPS, not only enhances the neurological function index, but also boosts nerve conduction velocity and the quantity of regenerated myelinated nerve fibers [65]. Furthermore, the utilization of the Radix Hedysari extract greatly improves the growth of lateral buds in proximal nerve stumps, and stimulates the amplification effect in the regeneration of peripheral nerves [66]. Moreover, HPS therapy in a mouse model of diabetic peripheral neuropathy has been shown to enhance the production of nerve growth factor and activate Nrf2 signaling. As a result, it reduces the level of Keap1, boosts motor nerve conduction speed, reduces the time taken for thermal withdrawal, and suppresses serum and oxidative stress in the sciatic nerve. Consequently, it leads to an improvement in diabetic peripheral neuropathy [67].

Another important component of MFRH is *Epimedium*. Previous research has demonstrated that the utilization of *Epimedium* in the treatment of sciatic nerve crush injury in rats has a significant impact on enhancing nerve regeneration and restoring the functionality of the injured nerve [68]. Local application of *Epimedium* significantly improved the conduction velocity and myelinated fiber count in rats with a 5 mm defect in the sciatic nerve [69]. *Epimedium* contains the primary bioactive flavonoid called icariin, which is a prenyl flavonol glycoside with pharmacological properties. Icariin has antineuroinflammatory, antiapoptotic, antioxidant, and neurogenesis-promoting effects and can treat different neurodegenerative and neuropsychiatric diseases, aging, and radiation-induced brain injury [70]. By modulating various signaling pathways, such as the PI3K/AKT, TGF β 1/Smad2, p38/MAPK, and Wnt pathways [71], icariin and its derivatives stimulate the activation of innate stem cells, enhance the growth of endothelial cells and smooth muscle cells, and facilitate nerve regeneration. Through the pathway of mitochondrial apoptosis, icariin hinders the activity of proinflammatory elements, oxidative stress, and neuronal cell death. Additionally, it notably improves the restoration of motor function in mice suffering from spinal cord injury [72]. The administration of icariin to a rat model with spinal cord injury reduced the expression and activity of proapoptotic proteins, elevated the level of antiapoptotic proteins, mitigated oxidative stress reactions, lowered the level of inflammatory molecules, enhanced the expression of anti-inflammatory proteins, reduced spinal cord edema, and greatly facilitated the restoration of motor function [73]. Application of total flavone of *Epimedium* to a cuprizone-induced demyelination mouse model increases the enrichment of astrocytes in the corpus callosum, striatum, and cortex, promotes expression of neurotrophic factors by astrocytes, and decreases

astrocyte expression of platelet-activating factor receptor (PAFR), which suppresses astrocyte-derived inflammatory responses, thereby contributing to myelin protection and regeneration [74]. By inhibiting the IRE1 α -XBP1 signaling pathway, icariin relieves neuronal apoptosis caused by endoplasmic reticulum stress following oxygen-glucose deprivation/reperfusion injury [75].

In addition to Radix Hedysari and *Epimedium* another component in MFRH is *Lumbricus*. *Lumbricus* has pro-regenerative properties that can help regenerate severed body parts [76]. For centuries, *Lumbricus* has been utilized in China to enhance nerve function. In a previous investigation, the administration of *Lumbricus* extract greatly enhanced the restoration of the neurological function index and nerve conduction velocities in rats suffering from sciatic nerve crush injury [77]. The utilization of *Lumbricus* extract as an auxiliary treatment method, and the proximal common peroneal nerve as a donor nerve connection significantly improved the nerve conduction velocities, morphological measurement results, histological analyses, and amplification effect [78]. The findings indicate that the capacity of MFRH to enhance nerve regeneration is intricate and involves various mechanisms, providing a novel potential approach for the clinical treatment of peripheral nerve injuries.

The current research is preliminary and possesses certain constraints that necessitate additional research in the forthcoming period. First, in this study, only one conduit size was prepared, only one transposition repair model was employed, and only a portion of the distal nerve was examined. Henceforth, we shall investigate novel approaches for nerve transposition repair, create more personalized conduits, and conduct a more comprehensive assessment of the reparative outcome. Second, in this study, MFRH was prepared in the form of a solution. In the future, Different techniques could be used to prepare MFRH in various forms, such as powder, capsules, and tablets, or to formulate it into sustained-release or controlled-release formulations. Different formulations may exhibit different levels of activity. The study of appropriate formulations for nerve repair is of great clinical importance. Third, this study solely examined the impact of MFRH on enhancing nerve regeneration, without delving into the investigation of MFRH's active constituents and mode of operation. Henceforth, there will be endeavors to determine particular active components of MFRH, analyze the pharmacokinetics of MFRH, and explore the molecular mechanisms underlying the effect of MFRH. Moreover, in addition to the points mentioned above, this study solely examined the impacts of MFRH 16 weeks after surgery, thus necessitating additional studies to examine its effects over a more extended period.

5. Conclusions

A combination of chitosan-based conduits possessing different inner diameters and MFRH can considerably pro-

mote the regeneration and functional recovery of damaged nerves, which in turn enhances nerve transposition repair efficacy. The utilization of this method holds immense promise in the clinical treatment of severe injuries to peripheral nerves, and could aid in the advancement of more efficient approaches for treatment.

Availability of Data and Materials

The data are available from the corresponding author upon reasonable request.

Author Contributions

FSZ, QCL and YHK completed the conceptualization. BM completed the methodology. MZ and BM completed the software. FSZ, QCL and YHK completed the validation. MZ and YHK completed the formal analysis. BM completed the investigation. MZ and BM completed the resources. FSZ and YHK completed the data curation. QCL completed the writing—original draft preparation. FSZ and QCL completed the writing—review and editing. FSZ and MZ completed the visualization. YHK completed the supervision, project administration and funding acquisition. All authors have read and agreed to the published version of the manuscript. All authors contributed to editorial changes in the manuscript. All authors read and approved the final manuscript. All authors have participated sufficiently in the work to take public responsibility for appropriate portions of the content and agreed to be accountable for all aspects of the work in ensuring that questions related to its accuracy or integrity.

Ethics Approval and Consent to Participate

The animal protocols and treatment followed the Guidelines for Ethical Review of Experimental Animals for Animal Welfare, as outlined by the Ethics Committee and Experimental Animal Center of Peking University People's Hospital in Beijing, China. The study obtained an approved permit, with permit number 2022PHE050. Animal surgeries and care adhered to the standards of the National Institutes of Health Guide for the Care and Use of Laboratory Animals (NIH Publication No. 85-23, revised 1985). Information about the animals was displayed in accordance with the ARRIVE 2.0 guidelines.

Acknowledgment

We are grateful for the assistance of Figdraw (www.figdraw.com) in the construction of some of the illustrations.

Funding

This work was supported by the National Natural Science Foundation of China (32371048, 81971177), Key Laboratory of Trauma and Neural Regeneration (BMU2021XY008-03), and National Center for Trauma Medicine (BMU2021XY008-01).

Conflict of Interest

The authors declare no conflict of interest.

References

- [1] Cattin AL, Burden JJ, Van Emmenis L, Mackenzie FE, Hoving JJA, Garcia Calavia N, *et al.* Macrophage-Induced Blood Vessels Guide Schwann Cell-Mediated Regeneration of Peripheral Nerves. *Cell*. 2015; 162: 1127–1139.
- [2] Zhang M, An H, Gu Z, Huang Z, Zhang F, Wen Y, *et al.* Mimosin-Inspired Stimuli-Responsive Curling Bioadhesive Tape Promotes Peripheral Nerve Regeneration. *Advanced Materials*. 2023; e2212015.
- [3] Yuan Y, Li D, Yu F, Kang X, Xu H, Zhang P. Effects of Akt/mTOR/p70S6K Signaling Pathway Regulation on Neuron Remodeling Caused by Translocation Repair. *Frontiers in Neuroscience*. 2020; 14: 565870.
- [4] Zhang M, Li C, Liu SY, Zhang FS, Zhang PX. An electroencephalography-based human-machine interface combined with contralateral C7 transfer in the treatment of brachial plexus injury. *Neural Regeneration Research*. 2022; 17: 2600–2605.
- [5] Peixun Z, Na H, Kou Y, Xiaofeng Y, Jiang B. Peripheral nerve intersectional repair by bi-directional induction and systematic remodelling: biodegradable conduit tubulization from basic research to clinical application. *Artificial Cells, Nanomedicine, and Biotechnology*. 2017; 45: 1464–1466.
- [6] Fadia NB, Bliley JM, DiBernardo GA, Crammond DJ, Schilling BK, Sivak WN, *et al.* Long-gap peripheral nerve repair through sustained release of a neurotrophic factor in nonhuman primates. *Science Translational Medicine*. 2020; 12: eaav7753.
- [7] Jiang BG, Yin XF, Zhang DY, Fu ZG, Zhang HB. Maximum number of collaterals developed by one axon during peripheral nerve regeneration and the influence of that number on reinnervation effects. *European Neurology*. 2007; 58: 12–20.
- [8] Jiang B, Zhang P, Jiang B. Advances in small gap sleeve bridging peripheral nerve injury. *Artificial Cells, Blood Substitutes, and Immobilization Biotechnology*. 2010; 38: 1–4.
- [9] Yin XF, Kou YH, Wang YH, Zhang P, Zhang HB, Jiang BG. Portion of a nerve trunk can be used as a donor nerve to reconstruct the injured nerve and donor site simultaneously. *Artificial Cells, Blood Substitutes, and Immobilization Biotechnology*. 2011; 39: 304–309.
- [10] Zhang P, Kou Y, Yin X, Wang Y, Zhang H, Jiang B. The experimental research of nerve fibers compensation amplification innervation of ulnar nerve and musculocutaneous nerve in rhesus monkeys. *Artificial Cells, Blood Substitutes, and Immobilization Biotechnology*. 2011; 39: 39–43.
- [11] Yuan YS, Niu SP, Yu YL, Zhang PX, Yin XF, Han N, *et al.* Reinnervation of spinal cord anterior horn cells after median nerve repair using transposition with other nerves. *Neural Regeneration Research*. 2019; 14: 699–705.
- [12] Younes I, Rinaudo M. Chitin and chitosan preparation from marine sources. Structure, properties and applications. *Marine Drugs*. 2015; 13: 1133–1174.
- [13] Zhang M, Zhang F, Li C, An H, Wan T, Zhang P. Application of Chitosan and Its Derivative Polymers in Clinical Medicine and Agriculture. *Polymers*. 2022; 14: 958.
- [14] Moran HBT, Turley JL, Andersson M, Lavelle EC. Immunomodulatory properties of chitosan polymers. *Biomaterials*. 2018; 184: 1–9.
- [15] Aghbashlo M, Amiri H, Moosavi Basri SM, Rastegari H, Lam SS, Pan J, *et al.* Tuning chitosan's chemical structure for enhanced biological functions. *Trends in Biotechnology*. 2023; 41: 785–797.
- [16] Liu H, Wen W, Hu M, Bi W, Chen L, Liu S, *et al.* Chitosan

- conduits combined with nerve growth factor microspheres repair facial nerve defects. *Neural Regeneration Research*. 2013; 8: 3139–3147.
- [17] Zhang Y, Jiang Z, Wang Y, Xia L, Yu S, Li H, *et al.* Nerve Regeneration Effect of a Composite Bioactive Carboxymethyl Chitosan-Based Nerve Conduit with a Radial Texture. *Molecules*. 2022; 27: 9039.
- [18] Zhou G, Chen Y, Dai F, Yu X. Chitosan-based nerve guidance conduit with microchannels and nanofibers promotes schwann cells migration and neurite growth. *Colloids and Surfaces B: Biointerfaces*. 2023; 221: 112929.
- [19] Zhao Y, Wang Y, Gong J, Yang L, Niu C, Ni X, *et al.* Chitosan degradation products facilitate peripheral nerve regeneration by improving macrophage-constructed microenvironments. *Biomaterials*. 2017; 134: 64–77.
- [20] Boecker A, Daeschler SC, Kneser U, Harhaus L. Relevance and Recent Developments of Chitosan in Peripheral Nerve Surgery. *Frontiers in Cellular Neuroscience*. 2019; 13: 104.
- [21] Jiang B, Zhang P, Zhang D, Fu Z, Yin X, Zhang H. Study on small gap sleeve bridging peripheral nerve injury. *Artificial Cells, Blood Substitutes, and Immobilization Biotechnology*. 2006; 34: 55–74.
- [22] Kou YH, Yu YL, Zhang YJ, Han N, Yin XF, Yuan YS, *et al.* Repair of peripheral nerve defects by nerve transposition using small gap bio-sleeve suture with different inner diameters at both ends. *Neural Regeneration Research*. 2019; 14: 706–712.
- [23] Wang Y, Li J, Wo Y, Zhou Z. Panaxydol derived from Panax notoginseng promotes nerve regeneration after sciatic nerve transection in rats. *Journal of Integrative Neuroscience*. 2022; 21: 109.
- [24] Hussain G, Wang J, Rasul A, Anwar H, Qasim M, Zafar S, *et al.* Current Status of Therapeutic Approaches against Peripheral Nerve Injuries: A Detailed Story from Injury to Recovery. *International Journal of Biological Sciences*. 2020; 16: 116–134.
- [25] Lu Y, Yang J, Wang X, Ma Z, Li S, Liu Z, *et al.* Research progress in use of traditional Chinese medicine for treatment of spinal cord injury. *Biomedicine and Pharmacotherapy*. 2020; 127: 110136.
- [26] Wang ZY, Zhang PX, Han N, Kou YH, Yin XF, Jiang BG. Effect of Modified Formula Radix Hedysari on the Amplification Effect during Peripheral Nerve Regeneration. *Evidence-Based Complementary and Alternative Medicine*. 2013; 2013: 647982.
- [27] Li C, Zhang M, Liu SY, Zhang FS, Wan T, Ding ZT, *et al.* Chitin Nerve Conduits with Three-Dimensional Spheroids of Mesenchymal Stem Cells from SD Rats Promote Peripheral Nerve Regeneration. *Polymers*. 2021; 13: 3957.
- [28] Bain JR, Mackinnon SE, Hunter DA. Functional evaluation of complete sciatic, peroneal, and posterior tibial nerve lesions in the rat. *Plastic and Reconstructive Surgery*. 1989; 83: 129–138.
- [29] Lu CF, Wang B, Zhang PX, Han S, Pi W, Kou YH, *et al.* Combining chitin biological conduits with small autogenous nerves and platelet-rich plasma for the repair of sciatic nerve defects in rats. *CNS Neuroscience & Therapeutics*. 2021; 27: 805–819.
- [30] Zhang PX, Han N, Kou YH, Zhu QT, Liu XL, Quan DP, *et al.* Tissue engineering for the repair of peripheral nerve injury. *Neural Regeneration Research*. 2019; 14: 51–58.
- [31] Barnes SL, Miller TA, Simon NG. Traumatic peripheral nerve injuries: diagnosis and management. *Current Opinion in Neurology*. 2022; 35: 718–727.
- [32] Pi W, Zhang Y, Li L, Li C, Zhang M, Zhang W, *et al.* Polydopamine-coated polycaprolactone/carbon nanotube fibrous scaffolds loaded with brain-derived neurotrophic factor for peripheral nerve regeneration. *Biofabrication*. 2022; 14: 10.1088/1758-5090/ac57a6.
- [33] Rao F, Wang Y, Zhang D, Lu C, Cao Z, Sui J, *et al.* Aligned chitosan nanofiber hydrogel grafted with peptides mimicking bioactive brain-derived neurotrophic factor and vascular endothelial growth factor repair long-distance sciatic nerve defects in rats. *Theranostics*. 2020; 10: 1590–1603.
- [34] Deng JX, Zhang DY, Li M, Weng J, Kou YH, Zhang PX, *et al.* Autologous transplantation with fewer fibers repairs large peripheral nerve defects. *Neural Regeneration Research*. 2017; 12: 2077–2083.
- [35] Faroni A, Mobasser SA, Kingham PJ, Reid AJ. Peripheral nerve regeneration: experimental strategies and future perspectives. *Advanced Drug Delivery Reviews*. 2015; 82–83: 160–167.
- [36] Kou Y, Zhang P, Yin X, Wei S, Wang Y, Zhang H, *et al.* Influence of different distal nerve degeneration period on peripheral nerve collateral sprouts regeneration. *Artificial Cells, Blood Substitutes, and Immobilization Biotechnology*. 2011; 39: 223–227.
- [37] Qi Z, Li D, Li L, Meng D, Deng J, Jin B, *et al.* Studies on the Manner of Collateral Regeneration From Nerve Stem to Motor Endplate. *Frontiers in Physiology*. 2022; 12: 795623.
- [38] Yin XF, Kou YH, Wang YH, Zhang P, Zhang DY, Fu ZG, *et al.* Can “dor to dor+rec neurorrhaphy” by biodegradable chitin conduit be a new method for peripheral nerve injury? *Artificial Cells, Blood Substitutes, and Immobilization Biotechnology*. 2011; 39: 110–115.
- [39] Yu Y, Zhang P, Han N, Kou Y, Yin X, Jiang B. Collateral development and spinal motor reorganization after nerve injury and repair. *American Journal of Translational Research*. 2016; 8: 2897–2911.
- [40] Yu F, Yu YL, Niu SP, Zhang PX, Yin XF, Han N, *et al.* Repair of long segmental ulnar nerve defects in rats by several different kinds of nerve transposition. *Neural Regeneration Research*. 2019; 14: 692–698.
- [41] Modrak M, Talukder MAH, Gurgenshvilvi K, Noble M, Elfars JC. Peripheral nerve injury and myelination: Potential therapeutic strategies. *Journal of Neuroscience Research*. 2020; 98: 780–795.
- [42] Pi W, Li C, Zhang M, Zhang W, Zhang PX. Myelin-associated glycoprotein combined with chitin conduit inhibits painful neuroma formation after sciatic nerve transection. *Neural Regeneration Research*. 2022; 17: 1343–1347.
- [43] Yin X, Zhang X, Kou Y, Wang Y, Zhang L, Jiang B, *et al.* How many nerve fibres can be separated as donor from an integral nerve trunk when reconstructing a peripheral nerve trauma with amplification method by artificial biochitin conduit? *Artificial Cells, Nanomedicine, and Biotechnology*. 2018; 46: 646–651.
- [44] Kou Y, Peng J, Wu Z, Yin X, Zhang P, Zhang Y, *et al.* Small gap sleeve bridging can improve the accuracy of peripheral nerve selective regeneration. *Artificial Cells, Nanomedicine, and Biotechnology*. 2013; 41: 402–407.
- [45] Zhang PX, Li-Ya A, Kou YH, Yin XF, Xue F, Han N, *et al.* Biological conduit small gap sleeve bridging method for peripheral nerve injury: regeneration law of nerve fibers in the conduit. *Neural Regeneration Research*. 2015; 10: 71–78.
- [46] Liu S, Liu Y, Zhou L, Li C, Zhang M, Zhang F, *et al.* XT-type DNA hydrogels loaded with VEGF and NGF promote peripheral nerve regeneration via a biphasic release profile. *Biomaterials Science*. 2021; 9: 8221–8234.
- [47] Yu F, Yuan Y, Xu H, Niu S, Han N, Zhang Y, *et al.* Neutrophil peptide-1 promotes the repair of sciatic nerve injury through the expression of proteins related to nerve regeneration. *Nutritional Neuroscience*. 2022; 25: 631–641.
- [48] Lopes B, Sousa P, Alvites R, Branquinho M, Sousa AC, Mendonça C, *et al.* Peripheral Nerve Injury Treatments and Advances: One Health Perspective. *International Journal of Molecular Sciences*. 2022; 23: 918.
- [49] Jiang BG, Han N, Rao F, Wang YL, Kou YH, Zhang PX. Advance of Peripheral Nerve Injury Repair and Reconstruction.

- Chinese Medical Journal. 2017; 130: 2996–2998.
- [50] Kuffler DP, Foy C. Restoration of Neurological Function Following Peripheral Nerve Trauma. *International Journal of Molecular Sciences*. 2020; 21: 1808.
- [51] Wang ZY, Qin LH, Zhang WG, Zhang PX, Jiang BG. Qian-Zheng-San promotes regeneration after sciatic nerve crush injury in rats. *Neural Regeneration Research*. 2019; 14: 683–691.
- [52] Sun K, Fan J, Han J. Ameliorating effects of traditional Chinese medicine preparation, Chinese materia medica and active compounds on ischemia/reperfusion-induced cerebral microcirculatory disturbances and neuron damage. *Acta Pharmaceutica Sinica B*. 2015; 5: 8–24.
- [53] Gan L, Qian M, Shi K, Chen G, Gu Y, Du W, *et al.* Restorative effect and mechanism of mecobalamin on sciatic nerve crush injury in mice. *Neural Regeneration Research*. 2014; 9: 1979–1984.
- [54] Zhang PX, Yin XF, Kou YH, Xue F, Han N, Jiang BG. Neural regeneration after peripheral nerve injury repair is a system remodelling process of interaction between nerves and terminal effector. *Neural Regeneration Research*. 2015; 10: 52.
- [55] Li C, Liu SY, Pi W, Zhang PX. Cortical plasticity and nerve regeneration after peripheral nerve injury. *Neural Regeneration Research*. 2021; 16: 1518–1523.
- [56] Yuan YS, Xu HL, Liu ZD, Kou YH, Jin B, Zhang PX. Brain functional remodeling caused by sciatic nerve transection repair in rats identified by multiple-model resting-state blood oxygenation level-dependent functional magnetic resonance imaging analysis. *Neural Regeneration Research*. 2022; 17: 418–426.
- [57] Liu J, Deng W, Fan L, Tian L, Jin L, Jin Z, *et al.* The role of radix hedysari polysaccharide on the human umbilical vein endothelial cells (HUVECs) induced by high glucose. *European Journal of Internal Medicine*. 2012; 23: 287–292.
- [58] Sun WM, Wang YP, Duan YQ, Shang HX, Cheng WD. Radix Hedysari polysaccharide suppresses lipid metabolism dysfunction in a rat model of non-alcoholic fatty liver disease via adenosine monophosphate-activated protein kinase pathway activation. *Molecular Medicine Reports*. 2014; 10: 1237–1244.
- [59] Yu S, Zhang W, Yu J, Feng S, Guo T, Lu H. Inhibiting effect of Radix Hedysari Polysaccharide (HPS) on endotoxin-induced uveitis in rats. *International Immunopharmacology*. 2014; 21: 361–368.
- [60] Yang X, Xue Z, Fang Y, Liu X, Yang Y, Shi G, *et al.* Structure-immunomodulatory activity relationships of Hedysarum polysaccharides extracted by a method involving a complex enzyme combined with ultrasonication. *Food & Function*. 2019; 10: 1146–1158.
- [61] Xue Z, Shi G, Fang Y, Liu X, Zhou X, Feng S, *et al.* Protective effect of polysaccharides from Radix Hedysari on gastric ulcers induced by acetic acid in rats. *Food & Function*. 2019; 10: 3965–3976.
- [62] Shi G, Wang D, Xue Z, Zhou X, Fang Y, Feng S, *et al.* The amelioration of ulcerative colitis induced by Dinitrobenzenesulfonic acid with Radix Hedysari. *Journal of Food Biochemistry*. 2020; e13421.
- [63] Mo X, Guo D, Jiang Y, Chen P, Huang L. Isolation, structures and bioactivities of the polysaccharides from Radix Hedysari: A review. *International Journal of Biological Macromolecules*. 2022; 199: 212–222.
- [64] Wei D, Chen T, Yan M, Zhao W, Li F, Cheng W, *et al.* Synthesis, characterization, antioxidant activity and neuroprotective effects of selenium polysaccharide from Radix hedysari. *Carbohydrate Polymers*. 2015; 125: 161–168.
- [65] Wei SY, Zhang PX, Han N, Dang Y, Zhang HB, Zhang DY, *et al.* Effects of Hedysari polysaccharides on regeneration and function recovery following peripheral nerve injury in rats. *The American Journal of Chinese Medicine*. 2009; 37: 57–67.
- [66] Wang Z, Zhang P, Kou Y, Yin X, Han N, Jiang B. Hedysari extract improves regeneration after peripheral nerve injury by enhancing the amplification effect. *PLoS One*. 2013; 8: e67921.
- [67] He L, Huan P, Xu J, Chen Y, Zhang L, Wang J, *et al.* Hedysarum polysaccharide alleviates oxidative stress to protect against diabetic peripheral neuropathy via modulation of the keap1/Nrf2 signaling pathway. *Journal of Chemical Neuroanatomy*. 2022; 126: 102182.
- [68] Kou Y, Wang Z, Wu Z, Zhang P, Zhang Y, Yin X, *et al.* *Epimedium* extract promotes peripheral nerve regeneration in rats. *Evidence-Based Complementary and Alternative Medicine*. 2013; 2013: 954798.
- [69] Chen B, Niu SP, Wang ZY, Wang ZW, Deng JX, Zhang PX, *et al.* Local administration of icariin contributes to peripheral nerve regeneration and functional recovery. *Neural Regeneration Research*. 2015; 10: 84–89.
- [70] Li LR, Sethi G, Zhang X, Liu CL, Huang Y, Liu Q, *et al.* The neuroprotective effects of icariin on ageing, various neurological, neuropsychiatric disorders, and brain injury induced by radiation exposure. *Aging*. 2022; 14: 1562–1588.
- [71] Niu Y, Lin G, Pan J, Liu J, Xu Y, Cai Q, *et al.* Deciphering the myth of icariin and synthetic derivatives in improving erectile function from a molecular biology perspective: a narrative review. *Translational Andrology and Urology*. 2022; 11: 1007–1022.
- [72] Li H, Zhang X, Zhu X, Qi X, Lin K, Cheng L. The Effects of Icariin on Enhancing Motor Recovery Through Attenuating Pro-inflammatory Factors and Oxidative Stress via Mitochondrial Apoptotic Pathway in the Mice Model of Spinal Cord Injury. *Frontiers in Physiology*. 2018; 9: 1617.
- [73] Jia G, Zhang Y, Li W, Dai H. Neuroprotective role of icariin in experimental spinal cord injury via its antioxidant, anti-neuroinflammatory and anti-apoptotic properties. *Molecular Medicine Reports*. 2019; 20: 3433–3439.
- [74] Meng-Ru Z, Ruo-Xuan S, Ming-Yang Y, Tong T, Lei Z, Ying-Bo Y, *et al.* Antagonizing astrocytic platelet activating factor receptor-neuroinflammation for total flavone of epimedium in response to cuprizone demyelination. *International Immunopharmacology*. 2021; 101: 108181.
- [75] Mo ZT, Liao YL, Zheng J, Li WN. Icariin protects neurons from endoplasmic reticulum stress-induced apoptosis after OGD/R injury via suppressing IRE1 α -XBP1 signaling pathway. *Life Sciences*. 2020; 255: 117847.
- [76] Krause TL, Bittner GD. Rapid morphological fusion of severed myelinated axons by polyethylene glycol. *Proceedings of the National Academy of Sciences of the United States of America*. 1990; 87: 1471–1475.
- [77] Wei S, Yin X, Kou Y, Jiang B. Lumbricus extract promotes the regeneration of injured peripheral nerve in rats. *Journal of Ethnopharmacology*. 2009; 123: 51–54.
- [78] Zhang P, Wang Z, Kou Y, Han N, Xu C, Yin X, *et al.* Role of lumbricus extract in the nerve amplification effect during peripheral nerve regeneration. *American Journal of Translational Research*. 2014; 6: 876–885.